Hydrodynamic characteristics of an oscillating water column device – revisited

Richard Porter

School of Mathematics, Fry Building, Woodland Road, Bristol, BS8 1UG

September 26, 2025

Abstract

It has been 30 years since Evans & Porter ("Hydrodynamic characteristics of an oscillating water column device", Applied Ocean Research, vol. 17(3), 1995) was published. It is my most heavily cited paper with 500 citations according to Google Scholar. However, it is not particularly well written, contains errors and is not easy to understand. The paper assumes familiarity with some fundamental, yet quite obscure, mathematical results originating from the theory of wave energy developed in the 1970s and concentrates primarily on the mathematical method of solution rather than the practical implications of the results. Most shockingly of all the paper fails to include results that it should and has the potential to be misunderstood by other researchers. This work is an attempt to rectify these flaws.

1 Introduction

An Oscillating Water Column (OWC) wave energy converter (WEC) device exploits the resonance of a horizontally confined body of water with a free surface, connected to the rest of the ocean through a lower opening, to generate useful power. The volume of air trapped above the internal free surface is pumped back-and-forth through an air turbine as the water within the column rises and falls due to the passing of ocean waves.

The concept of an OWC precedes mainstream research into harnessing the power of ocean waves as a renewable energy source. The earliest known example dates back to the 1880s used as audible navigation aids, known as 'whistling buoys' off the coast of the USA [10]. In 1947 Yoshio Masuda designed a floating buoy equipped with a unidirectional turbine to generate electricity to power navigation lights [9]. Despite its low power output the use of OWCs to power navigational buoys remains the OWCs most widespread commercial success [10].

A small number of OWCs have been used to supply energy to national energy grids. In the UK, the LIMPET device installed on the Scottish Island of Islay operated from 2001 to 2011 and was rated at 125kW. In the Azores, the PICO plant (see, for example, [7]) operated from 1999 to 2018 until it was destroyed in a storm. Less well known is the Kvaerner OWC installed in Norway in 1985 (see for example, [8]) but destroyed in a storm four year later. It was located at one end of a natural harbour, a design theorised to produce a multi-resonant effect with the aim of increasing the bandwidth. The examples listed above involve installations into a shoreline location and are site specific. More recently, a number of projects in Japan,

India, China and Spain have involved installing smaller modular OWC units into sea walls to serve a dual purpose of coastal protection and energy generation. To date, the largest and most successful of these is the Mutriku Wave Power Plant, built in 2011 on the northern coast of Spain. It is comprised of 16 OWCs set up side-by-side in a harbour wall and has since supplied over 3GWh to the national electricity grid [12].

Early, but instructive work on the OWC concept such as that described by Evans [2] in 1978 applied rigid-body theory to a simple OWC model. By modelling the internal free surface as a weightless piston, it was demonstrated that the resonant motion of the fluid within the internal chamber can be excited at certain incident wave frequencies. Soon afterwards, [5] accounted for the internal free surface correctly using a theory based on oscillating pressure variations within the OWC device. This led to the general theoretical framework for multiple interacting OWCs described by Evans [3]. Some years later Evans & Porter [4], revisiting a problem initially considered by Smith [18], showed how a simple two-dimensional model of a shore-mounted OWC could extract 100% of the incoming wave energy at isolated resonant frequency dependent on the size and shape of the rectangular internal chamber [10]. In that work, the main focus of attention was given to the method of solution, specifically adapting the methods that had been developed in Porter & Evans [17] to derive fast accurate computations of the key hydrodynamic quantities that govern the operation of the particular OWC design. This was done with the focus on time-dependent modelling which requires information about the frequency-domain problem over the whole positive range of frequencies. Much less attention was given to the results to the extent that only curves of *maximum* efficiency as a function of wave frequency were presented rather than the variation of efficiency assuming *fixed* (i.e. not frequency-dependent) control parameters.

This omission is potentially significant for subsequent studies. In the experimental wave tank study undertaken by Morris-Thomas *et al.* [14] based on the design of Evans & Porter [17], the authors report a reduction in the efficiency of about a third from the theoretical maximum efficiency and hypothesize that viscous/turbulent losses are to blame. This may well be the case. But it is equally likely that the power take-off mechanism used by Morris-Thomas *et al.* [14] "modeled by a rectangular vent, of width 5mm, situated in the roof of the chamber" was never able to extract maximum efficiencies, at least not at every frequency. Clearly, Morris-Thomas *et al.* [14] knew this to be the case as they comment in their paper: "In altering the vent size, one could simulate different rates of energy extraction thus influencing the peak value of η_{max}" [the maximum efficiency] "However, this was not the focus of the present experiments." Thus, one purpose of this update of [4] is to present 'new' theoretical predictions for efficiency of power capture for a realistic model of air turbine power take off, including the effects of air compressibility. This might provide closer alignment between experiments and theory without having to rely on other physical effects to explain the discrepancies.

The primary reason for revisiting this work was in order to produce numerical results to add to the recent work of [15] Revisiting the work of my Ph.D made me realise how poorly the work in [4] was presented. By poor (and, by the way, I am not placing any blame upon my co-author here), I mean that the paper assumes a familiarity with the application of the mathematical theory of linearised water waves to wave energy extraction and leans quite heavily on the Ph.D thesis of [18] which I had access to but is not readily available to other researchers. So there are shortcuts which mean the work does not connect particularly well to the theory as it is described in modern textbooks. And, as has been explained, the theory did not include calculations of efficiency for different power control parameters. Finally, this work has given me a vehicle to document a much needed improvement to the general method described by [17] for

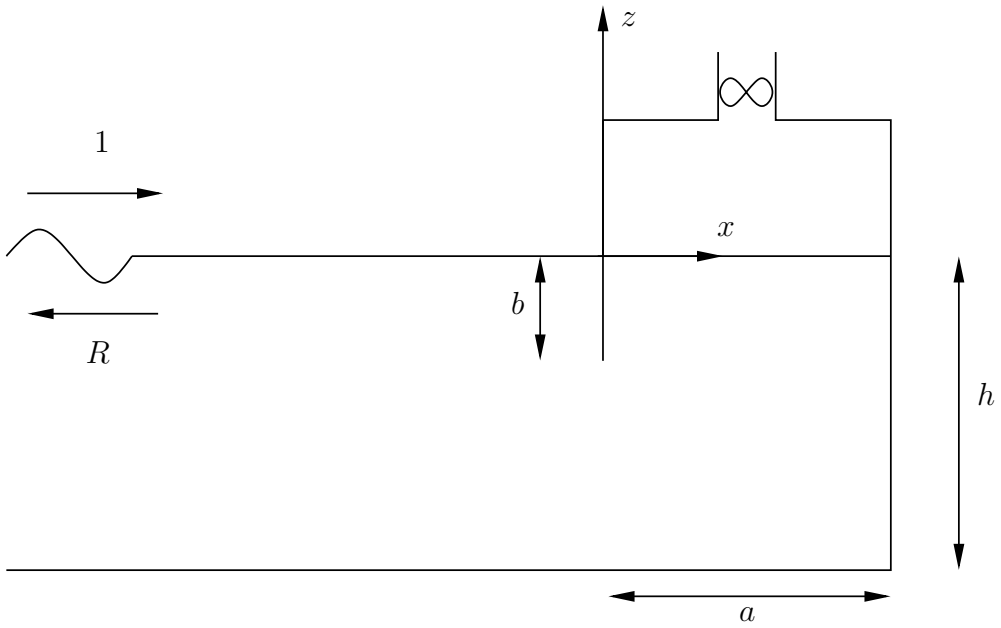

Figure 1: Definition sketch of the two-dimensional OWC.

problems involving vertical barriers. The current work also includes an updated and improved variation of the complementary method of solution outlined in the Ph.D thesis of Porter [16] but omitted from the paper of [4]

Coincidentally, I have been prompted by correspondance with Carlos Michelen Strofer who has pointed out typos and errors in the original [4] paper for which I am most grateful. No doubt I will have now introduced more errors and typos than I have corrected.

2 Definition of the problem

We consider the problem of two-dimensional waves propagating in the positive x-direction from $x = -\infty$ on fluid of density ρ a constant depth h. The front wall of the OWC is placed along $x = 0$ and extends a depth b below the mean free surface. The rear vertical wall of the OWC is placed along $x = a$, $-h < z < 0$, where z is directed upwards from an origin in the undisturbed free surface. When in motion, the oscillation of the internal free surface generates a time-varying pressure, $P_i(t)$, in the air chamber above which drives a volume flux of air denoted by $Q(t)$ through a self-rectifying air turbine to the external constant atmospheric pressure, P_a.

Under the assumptions of inviscid small-amplitude theory, the time-dependent problem maybe described by a velocity potential $\Phi(x, z, t)$ which satisfies

$$\nabla^2\Phi = 0 \tag{1}$$

in the fluid. On the bed, $z = -h$, $x < a$,

$$\Phi_z = 0. \tag{2}$$

On each side of fixed barriers and along the back wall we must also enforce a zero normal velocity condition so that

$$\Phi_x = 0, \qquad x = 0^{\pm},\ -b < z < 0 \tag{3}$$

and

$$\Phi_x = 0, \qquad x = a, \ -h < z < 0. \tag{4}$$

The surface of the fluid is represented by $\zeta(x,t)$ and satisfies a kinematic condition

$$\zeta_t = \Phi_z, \qquad z = 0, \ \{x < 0\} \cup \{0 < x < a\}. \tag{5}$$

Within the linearised fluid domain the pressure, $P(x,z,t)$, is given by the linearised Bernoulli equation

$$P(x,z,t) - P_a = -\rho\Phi_t - \rho g z. \tag{6}$$

Boundary conditions on the surface of the water are given, for $x < 0$, by $P(x,\zeta,t) = P_a$, whilst for $0 < x < a$, $P(x,\zeta,t) = P_i(t)$ so that

$$-\rho\Phi_t(x,0,t) - \rho g\zeta(x,t) = \begin{cases} P_i(t) - P_a, & 0 < x < a \\ 0, & x < 0. \end{cases} \tag{7}$$

to leading order. The volume flux of fluid across the internal free surface (and hence across the turbine) is assumed to be connected to the pressure in the air chamber above by the linear relationship

$$Q(t) = \lambda_1(P_i(t) - P_a) + \lambda_2 \frac{d}{dt} P_i(t) \tag{8}$$

where

$$Q(t) = \int_0^a \Phi_z(x,0,t)\,dx = \int_{-h}^{-b} \Phi_x(0,z,t)\,dz. \tag{9}$$

for $0 < x < a$. The equivalence of the last two integrals is a consequence of incompressibility (one can integrate $\nabla^2\phi$ over $(x,z) \in \{0 < x < a, \ -h < z < 0\}$ and use the divergence theorem). In (8), λ_1, λ_2 are positive real parameters which control the damping (see, for example, [6], or [13]. In particular, λ_2 accounts for the compressibility of air and is given by

$$\lambda_2 = \frac{V_0}{\rho_a c_a^2} \tag{10}$$

where ρ_a, c_a are the density of air and the speed of sound in air and V_0 is the volume of air (per unit length) in the chamber above the internal free surface. All are measured with respect to the static system. A formula for the parameter λ_1 can be expressed for a Well's-type turbine in terms of its geometry, but we assume this is a parameter we vary freely.

Finally we require conditions at infinity. A wave of amplitude A and frequency ω is incident from $x = -\infty$ and is partially reflected back towards $x = -\infty$. This can be expressed as

$$\Phi(x,z,t) \sim \Re\left\{ -\frac{\mathrm{i}gA}{\omega}(\mathrm{e}^{\mathrm{i}kx} + R\mathrm{e}^{-\mathrm{i}kx})\psi_0(z)\mathrm{e}^{-\mathrm{i}\omega t} \right\}, \qquad x \to -\infty \tag{11}$$

where R is the complex reflection coefficient, encoding modulus and phase, and

$$\psi_0(z) = \cosh k(z+h)/\cosh kh \tag{12}$$

is the depth variation associated with propagating waves; the wavenumber k is the solution of $k\tanh kh = K \equiv \omega^2/g$.

On account of the governing equations and boundary conditions being assumed linear, the system response shares the same frequency as the incident wave. We therefore factorise a harmonic time dependence from all dependent variables at the same time as non-dimemnsionalising by writing

$$(x, z, a, b, h) = K^{-1}(x', z', a', b', h'); \quad k = Kk' \tag{13}$$

with

$$\Phi(x, z, t) = \Re\left\{-\frac{\mathrm{i}gA}{\omega}\phi(x', z')\mathrm{e}^{-\mathrm{i}\omega t}\right\}, \qquad Q(t) = \Re\left\{-\frac{\mathrm{i}gA}{\omega}q\mathrm{e}^{-\mathrm{i}\omega t}\right\} \tag{14}$$

along with

$$\zeta(x, t) = \Re\{A\eta(x')\mathrm{e}^{-\mathrm{i}\omega t}\}, \qquad P_i(t) - P_a = \Re\left\{\rho g A p_i \mathrm{e}^{-\mathrm{i}\omega t}\right\}. \tag{15}$$

The boundary-value problem is now expressed (after dropping primes) as

$$\nabla^2\phi = 0, \qquad \text{in the fluid} \tag{16}$$

with the following no flow boundary conditions:

$$\phi_z(x, -h) = 0, \quad x < a, \quad \phi_x(0^{\pm}, z) = 0, \quad -b < z < 0; \quad \text{and} \quad \phi_x(a, z) = 0, \quad -h < z < 0. \tag{17}$$

Additionally, after the elimination of η, the conditions on $z = 0$ are expressed as

$$\phi - \phi_z = \begin{cases} 0, & x < 0, \\ p_i, & 0 < x < b. \end{cases} \tag{18}$$

Finally the turbine law (8) reduces to

$$q = \mathrm{i}\Lambda p_i \tag{19}$$

where

$$\Lambda = \rho\omega\lambda_1 - \mathrm{i}\rho\omega^2\lambda_2 \tag{20}$$

is a dimensionless (complex) control parameter and

$$q = \int_0^a \phi_z(x, 0)\, dx = \int_{-h}^{-b} \phi_x(0, z)\, dz. \tag{21}$$

The scaling used in (14) implies that

$$\phi(x, z) \sim (\mathrm{e}^{\mathrm{i}kx} + R\mathrm{e}^{-\mathrm{i}kx})\psi_0(z), \qquad x \to -\infty \tag{22}$$

where $\psi_0(z)$ is defined as before by (12) but noting that k now represents the *dimensionless* wavenumber satisfying

$$1 = k \tanh kh. \tag{23}$$

The mean power (i.e. time averaged over a period) per unit length, $\bar{W}$ extracted by the turbines can be calculated from the balance of flux of energy through a vertical boundary far from the device. In other words

$$\begin{aligned} \bar{W} &= \lim_{X\to-\infty}\left\{\frac{\omega}{2\pi}\int_0^{2\pi/\omega}\int_{-h}^{0}(-\rho\Phi_t(X, z, t))\Phi_x(X, z, t)\, dz\, dt\right\} \\ &= \lim_{X'\to-\infty}\frac{1}{2}\Re\left\{\mathrm{i}\omega\rho\int_{-h'}^{0}\left(-\frac{\mathrm{i}gA}{\omega}\phi(X', z')\right)\left(\frac{\mathrm{i}gA^*}{\omega}\phi^*_{x'}(X', z')\right)\, dz'\right\} \\ &= \bar{W}_{inc}E \end{aligned} \tag{24}$$

where $*$ denotes complex conjugation and where we used the definition (22) to derive

$$E = 1 - |R|^2. \tag{25}$$

Also in (24),

$$\bar{W}_{inc} = \frac{1}{2}\rho g|A|^2 c_g \tag{26}$$

represents the flux of energy per unit length associated with a plane-crested incident wave where

$$c_g = \frac{1}{2}\frac{g\tanh kh}{\omega}\left(1 + \frac{2kh}{\sinh 2kh}\right) \tag{27}$$

is the group velocity and uses the result

$$k\int_{-h}^{0}\psi_0^2(z)\,dz = \tanh kh\frac{1}{2}\left(1 + \frac{2kh}{\sinh 2kh}\right). \tag{28}$$

On account of (24), $E \in [0,1]$ as defined by (25) is the *efficiency*.

Alternatively, $\bar{W}$ can be calculated from the time average over a period of the rate of working of the pressure in driving flow across the turbine, or

$$\bar{W} = \frac{\omega}{2\pi}\int_0^{2\pi/\omega}(P_i(t) - P_a)Q(t)\,dt. \tag{29}$$

This expression, recast in terms of frequency-dependent dimensionless variables, is

$$\bar{W} = \frac{1}{2}\frac{\rho g^2|A|^2}{\omega}\Im\{qp_i^*\} \tag{30}$$

and so, using (19), (26) and (27) we find

$$E = \frac{g}{\omega c_g}|p_i^2|\Re\{\Lambda\} = \frac{|p_i^2|\Re\{\Lambda\}}{\frac{1}{2}(1 + 2kh/\sinh 2kh)\tanh kh} \tag{31}$$

provides an alternative expression for calculation the efficiency of the device.

The two expressions for E are formally the same, a fact which is established by using ϕ and ϕ^* in Green's identity over the whole of the fluid domain extending to $x = X$ (< 0) and letting $X \to -\infty$. This results in

$$2\mathrm{i}k(1 - |R|^2)\int_{-h}^{0}\psi_0^2(z)\,dz = 2\mathrm{i}\Im\{p_i^* q\} \tag{32}$$

from which equivalence of (25) and (25) can be established.

3 Solution

We first decompose the potential into a scattering and radiation potentials by writing

$$\phi(x,z) = \phi^S(x,z) + p_i\phi^R(x,z) \tag{33}$$

where $\phi^S(x,z)$ includes the incident wave but no pressure forcing on the internal free surface and $\phi^R(x,z)$ does the opposite. We write solutions in standard separation series (see [11]) so that in $x<0$

$$\phi^S(x,z) = (\mathrm{e}^{\mathrm{i}kx} + R^S\mathrm{e}^{-\mathrm{i}kx})\psi_0(z) + \sum_{n=1}^{\infty} a_n^S \mathrm{e}^{k_n x}\psi_n(z) \tag{34}$$

and

$$\phi^R(x,z) = A^R\mathrm{e}^{-\mathrm{i}kx}\psi_0(z) + \sum_{n=1}^{\infty} a_n^R \mathrm{e}^{k_n x}\psi_n(z) \tag{35}$$

where $a_n^{S,R}$ are coefficients, k_n $(n \geq 1)$ are the positive, real solutions of $k_n \tan k_n h = -1$ (ordered by increasing magnitude) and

$$\psi_n(z) = \cos k_n(z+h)/\cos k_n h \tag{36}$$

are the depth eigenfunctions. They satisfy the orthogonality relation

$$\frac{1}{h}\int_{-h}^{0} \psi_n(z)\psi_m(z)\,dz = N_n\delta_{mn} \tag{37}$$

for $m,n \geq 0$ where δ_{mn} is the Kronecker delta where we have extended the definition of k_n to include $k_0 \equiv -\mathrm{i}k$. Also in (37), we have defined

$$N_n = \frac{1}{2}\left(1 + \frac{\sin 2k_n h}{2k_n h}\right)\sec^2 k_n h \tag{38}$$

for $n \geq 0$. For $n=0$, this gives

$$N_0 = \frac{1}{2}\left(1 + \frac{\sinh 2kh}{2kh}\right)\mathrm{sech}^2 kh \tag{39}$$

and we note from (28) that

$$\omega c_g/g = khN_0. \tag{40}$$

From (22), (33)–(35) it is clear that

$$R = R^S + p_i A^R \tag{41}$$

and R^S, p_i and A^R are all coefficients to be found. These represent, respectively: the coefficient of reflection due to waves incident on a barrier next to a wall without a power take off mechanism in place; the amplitude of pressure variations of the internal air chamber; the waves radiated to infinity by an imposed oscillating pressure variation on the internal free surface.

We note that if we let $U^{S,R}(z) \equiv \phi_x^{S,R}(0,z)$ for $-h<z<-b$ then we may deduce, using (17) and (37), that

$$\mathrm{i}khN_0(1-R^S) = \int_{-h}^{-b} U^S(z)\psi_0(z)\,dz, \qquad \text{and} \qquad -\mathrm{i}khN_0A^R = \int_{-h}^{-b} U^R(z)\psi_0(z)\,dz \tag{42}$$

whilst

$$k_n h N_n a_n^{S,R} = \int_{-h}^{-b} U^{S,R}(z)\psi_n(z)\,dz. \tag{43}$$

Now we consider the region $0 < x < a$ (assuming temporarily that $ka \neq n\pi$, $n = 1, 2, \ldots$) and write

$$\phi^S(x,z) = \mathrm{i}(1-R^S)\frac{\cos k(x-a)}{\sin ka}\psi_0(z) - \sum_{n=1}^{\infty} a_n^S \frac{\cosh k_n(x-a)}{\sinh k_n a}\psi_n(z) \tag{44}$$

and

$$\phi^R(x,z) = 1 - \mathrm{i}A^R\frac{\cos k(x-a)}{\sin ka}\psi_0(z) - \sum_{n=1}^{\infty} a_n^R \frac{\cosh k_n(x-a)}{\sinh k_n a}\psi_n(z). \tag{45}$$

These expansions, written in terms of the unknown coefficients of (34) and (35) are designed to ensure continuity of $\phi_x^{S,R}(x,z)$ across $x = 0$, $-h < z < 0$ (the whole fluid depth) in addition to satisfying Laplace's equation, the Neumann wall condition along $x = a$ and the internal free surface conditions $\phi^S - \phi_z^S = 0$ and $\phi^R - \phi_z^R = 1$ on $z = 0$.

Ensuring continuity of pressure everywhere in the fluid requires us to match the values of $\phi^{S,R}$ given by (34) and (44) or (35) and (45) at their common interface $x = 0$ for $-h < z < -b$. For the scattering problem this results in

$$[\mathrm{i}(1-R^S)\cot ka - (1+R^S)]\psi_0(z) = (\mathcal{K}U^S)(z), \qquad -h < z < -b \tag{46}$$

where the integral operator is defined by

$$(\mathcal{K}U^S)(z) \equiv \int_{-h}^{-b} U^S(z')\kappa(z,z')\,dz' \tag{47}$$

having the kernel function

$$\kappa(z,z') = \sum_{n=1}^{\infty} \frac{(1+\coth k_n a)}{N_n k_n h}\psi_n(z)\psi_n(z'). \tag{48}$$

Likewise, for the radiation problem, we find

$$1 - (1+\mathrm{i}\cot ka)A^R\psi_0(z) = (\mathcal{K}U^R)(z), \qquad -h < z < -b. \tag{49}$$

We let $u_i(z)$ be the solution of

$$(\mathcal{K}u_i)(z) = f_i(z), \qquad -h < z < -b \tag{50}$$

$(i = 1, 2)$ where we have abbreviated

$$f_1(z) = 1, \qquad f_2(z) = \psi_0(z). \tag{51}$$

It follows that

$$U^S(z) = [\mathrm{i}(1-R^S)\cot ka - (1+R^S)]u_2(z) \tag{52}$$

and

$$U^R(z) = u_1(z) - (1+\mathrm{i}\cot ka)A^R u_2(z). \tag{53}$$

We also define the 2×2 matrix S to have entries

$$\mathsf{S}_{ij} = \frac{1}{khN_0}\int_{-h}^{-b} u_i(z)f_j(z)\,dz \tag{54}$$

$(i,j=1,2)$. On account of $\kappa(z,z')$ being real and symmetric ($\kappa(z,z')=\kappa(z',z)$) it follows that S is real and symmetric ($\mathsf{S}_{ij}=\mathsf{S}_{ji}$). It follows from using (52) in (42) that

$$\mathrm{i}(1-R^S)=[\mathrm{i}(1-R^S)\cot ka-(1+R^S)]\mathsf{S}_{22}. \tag{55}$$

Rearranging gives

$$R^S=-\frac{\mathsf{S}_{22}-\mathrm{i}(\mathsf{S}_{22}\cot ka-1)}{\mathsf{S}_{22}+\mathrm{i}(\mathsf{S}_{22}\cot ka-1)} \tag{56}$$

and shows that $|R^S|=1$, as required (energy is conserved in the scattering problem with no power take off). Following (33) and partitioning the flux

$$q=q^S+p_iq^R \tag{57}$$

means that

$$q^S=\int_{-h}^{-b}U^S(z)\,dz=[\mathrm{i}(1-R^S)\cot ka-(1+R^S)]khN_0\mathsf{S}_{21} \tag{58}$$

after using (21), (52). Combining (56) with (58) gives

$$q^S=\frac{2\mathrm{i}khN_0\mathsf{S}_{21}}{\mathsf{S}_{22}+\mathrm{i}(\mathsf{S}_{22}\cot ka-1)}. \tag{59}$$

We move onto the identities relating to the solution of the radiation problem. Thus, using (53) in (42) gives

$$-\mathrm{i}A^R=\mathsf{S}_{12}-(1+\mathrm{i}\cot ka)A^R\mathsf{S}_{22} \tag{60}$$

whence

$$A^R=\frac{\mathsf{S}_{12}}{\mathsf{S}_{22}+\mathrm{i}(\mathsf{S}_{22}\cot ka-1)} \tag{61}$$

Also, using (53) in (21) gives

$$q^R=khN_0\left[\mathsf{S}_{11}-(1+\mathrm{i}\cot ka)A^R\mathsf{S}_{21}\right] \tag{62}$$

whence we find

$$q^R=\frac{khN_0[(\mathrm{i}\cot ka+1)(\mathsf{S}_{11}\mathsf{S}_{22}-\mathsf{S}_{12}\mathsf{S}_{21})-\mathrm{i}\mathsf{S}_{11}]}{\mathsf{S}_{22}+\mathrm{i}(\mathsf{S}_{22}\cot ka-1)}. \tag{63}$$

The results above mimic those given in [4] with different scalings owing to the slightly different definitions used in this work.

In order to determine the remaining unknown, p_i, we use (19) with (57) so that

$$p_i=-\mathrm{i}q^S/(\Lambda+\mathrm{i}q^R). \tag{64}$$

3.1 Efficiency

Let us write

$$\mathrm{i}q^R=Z=B+\mathrm{i}D \tag{65}$$

so that $q^R=D-\mathrm{i}B$, where D, B real. The efficiency can be found using (64) in (31) so that

$$E=\frac{g}{\omega c_g}\frac{|q^S|^2\Re\{\Lambda\}}{|\Lambda+Z|^2}. \tag{66}$$

Then we use the general result assuming $\Lambda \in \mathbb{C}$

$$|\Lambda + Z|^2 - |\Lambda + Z^*|^2 = 4\Re\{\Lambda\}\Re\{Z\} \tag{67}$$

to show that

$$E = \frac{1}{khN_0}\frac{|q^S|^2}{4B}\left(1 - \frac{|\Lambda - Z^*|^2}{|\Lambda + Z|^2}\right) \tag{68}$$

after use is made of (40).

If, as is often assumed, $\Im\{\Lambda\} = 0$ then we can use a modified version of (67) to give

$$E = \frac{1}{khN_0}\frac{|q^S|^2}{2(\Re\{Z\} + |Z|)}\left(1 - \frac{(\Lambda - |Z|)^2}{|\Lambda + Z|^2}\right). \tag{69}$$

Separately, it can be shown using Green's identity over the fluid domain with the pair of functions ϕ^R and $(\phi^R)^*$ that

$$B = khN_0|A^R|^2 \tag{70}$$

(hence demonstrating that $B \geq 0$) and, with the pair of functions ϕ^S and ϕ^R, that

$$q^S = 2\mathrm{i}khN_0A^R. \tag{71}$$

We remark that this identity is clearly satisfied by (59) and (61). Combining these two results gives

$$4khN_0B = |q^S|^2. \tag{72}$$

Returning to (69) this means that in the case that Λ is complex

$$E = 1 - \frac{|\Lambda - B + \mathrm{i}D|^2}{|\Lambda + B + \mathrm{i}D|^2} \tag{73}$$

with maximum efficiency of $E = 1$ when $\Lambda = B - \mathrm{i}D = Z^*$. That is, for a given wave frequency we can find a Λ such that all incoming wave energy is captured provided $D \geq 0$ (this is because the real and imaginary parts of Λ are both non-negative).

In the case that Λ is real, we have

$$E = \frac{2B}{B + \sqrt{D^2 + B^2}}\left(1 - \frac{(\Lambda - \sqrt{D^2 + B^2})^2}{|\Lambda + B + \mathrm{i}D|^2}\right) \tag{74}$$

which obtains a maximum of

$$E_{max} = \frac{2B}{B + \sqrt{D^2 + B^2}} \tag{75}$$

when $\Lambda = \Lambda_{max} = (D^2 + B^2)^{1/2}$. This last result is derived in [4]. Clearly, $E_{max} = 1$ is possible iff $D = 0$ and $\Lambda = B$ simultaneously. It is not obvious from any preceding results that there should be frequencies for which $D = 0$.

The variation of E for *fixed* Λ was not considered in [4]; only curves of E_{max} were shown and only for Λ real.

3.2 Numerical approximation

In the previous section we have shown that the only quantity needed to determine the efficiency are the real and imaginary parts of the complex quantity $q^R = B - \mathrm{i}D$ where q^R is given by (62). Thus we require the 4 elements of the matrix S defined by (54) which rely on the solutions $u_1(z)$, $u_2(z)$ defined by the integral equation (50).

We employ the Galerkin method in which the solution to the integral equations are approximated by an expansion

$$u_i(z) \approx \sum_{p=0}^{P} \alpha_p^{(i)} w_{2p}\left(\frac{h+z}{h-b}\right), \qquad i = 1, 2, \tag{76}$$

for $-h < z < -b$ in terms of unknown coefficients $\alpha_p^{(i)}$ In (76) P is the truncation parameter and

$$w_{2p}(t) = \frac{2(-1)^p}{\pi(1-t^2)^{1/2}} T_{2p}(t) \tag{77}$$

define test functions in terms of the orthogonal Chebychev polynomials. The functions $w_{2p}(t)$ incorporate the inverse square root behaviour at the end point $t = 1$ associated with the known singularities in the velocity field at the end of the thin barriers and, being even in z, the no-flow condition on $z = -h$.

The Galerkin scheme applied to the integral equations (50) involves substituting (76) into (50), multiplying by $w_{2q}[(h+z)/(h-b)]$ for $q = 0, \ldots, P$ and integrating over $-h < z < -b$. The result is the linear system of equations

$$\sum_{p=0}^{P} \alpha_p^{(i)} \mathcal{K}_{pq} = F_{q0}^{(i)}, \qquad q = 0, \ldots, P \tag{78}$$

$(i = 1, 2)$ where

$$\mathcal{K}_{pq} = \sum_{n=1}^{\infty} \frac{(1 + \coth k_n a)}{N_n k_n h} F_{pn}^{(2)} F_{qn}^{(2)} \tag{79}$$

and

$$\begin{aligned} F_{pn}^{(2)} = \int_{-h}^{-b} w_{2p}\left(\frac{h+z}{h-b}\right) \psi_n(z)\, dz &= \sec k_n h \int_0^1 \frac{2(-1)^p T_{2p}(t)}{\pi\sqrt{1-t^2}} \cos k_n(h-b)t\, dt \\ &= \sec k_n h J_{2p}[k_n(h-b)] \end{aligned} \tag{80}$$

(see [1] §1.10(2)) Here $J_p(\cdot)$ denotes the Bessel function of order p. The result applies when $n = 0$ by making the substitution $k_0 = -\mathrm{i}k$ so that

$$F_{p0}^{(2)} = \operatorname{sech} kh (-1)^p I_{2p}[k(h-b)] \tag{81}$$

where $I_p(\cdot)$ denotes the modified Bessel function. Thus, the explicit version of (79) is

$$\mathcal{K}_{pq} = 4 \sum_{n=1}^{\infty} \frac{(1 + \coth k_n a)}{(2k_n h + \sin 2k_n h)} J_{2p}[k_n(h-b)] J_{2q}[k_n(h-b)] \tag{82}$$

which is real and symmetric. Terms in the series decay slowly (like $O(1/n^2)$ as $n \to \infty$) although there are ways of speeding this up (see [17] for example). The only other term needed in (78) is

$$F_{p0}^{(1)} = \int_{-h}^{-b} w_{2p}\left(\frac{h+z}{h-b}\right)\, dz = \delta_{p0} \tag{83}$$

and then using (76) in (54) gives

$$\mathsf{S}_{ij} \approx \tilde{\mathsf{S}}_{ij} = \frac{1}{khN_0}\sum_{p=0}^{P} \alpha_p^{(i)} F_{q0}^{(j)}, \tag{84}$$

$(i, j = 1, 2)$.

4 A complementary method of solution

An alternative formulation of the solution to the problem is possible resulting in integral equations defined over the depth interval occupied by the barrier (i.e. complementary to the interval over which integral equations were defined previously: the gaps not occupied by the barrier).

This alternative formulation was not presented in the paper of [4], although a version is documented in the Ph.D thesis of Porter [16]. Although less direct than the one already outlined it is nevertheless just a powerful and particularly well suited to barriers which are small compared to the depth. In what follows significant improvements are made to the original work described in [16].

We start by focusing on the scattering problem which is actually quite straightforward. From (34) and (44) we have

$$\begin{aligned}\left[\phi^S(x,z)\right]_{x=0^-}^{x=0^+} &= [\mathrm{i}(1-R^S)\cot ka - (1+R^S)]\psi_0(z) - \sum_{n=1}^{\infty} a_n^S(1+\coth k_n a)\psi_n(z) \\ &= \begin{cases} P^S(z), & -b < z < 0, \\ 0, & -h < z < -b \end{cases}\end{aligned} \tag{85}$$

where $P^S(z)$ encodes the unknown pressure jump across the barrier. Making use of orthogonality allows us to write

$$N_0 h[\mathrm{i}(1-R^S)\cot ka - (1+R^S)] = \int_{-b}^{0} P^S(z)\psi_0(z)\, dz \tag{86}$$

and

$$-N_n h a_n^S(1+\coth k_n a) = \int_{-b}^{0} P^S(z)\psi_n(z)\, dz. \tag{87}$$

The remaining condition to be imposed is that $\phi_x^S(0,z) = 0$ on $-b < z < 0$ which, using (34) and (78), results in

$$\mathrm{i}k(1-R^S)\psi_0(z) = \sum_{n=1}^{\infty} \frac{k_n}{N_n h(1+\coth k_n a)}\psi_n(z)\int_{-b}^{0} P^S(z')\psi_n(z')\, dz'. \tag{88}$$

The interchange of summation and integration is not allowed, although it is possible to write

$$\mathrm{i}k(1-R^S)\psi_0(z) = -\frac{d^2}{dz^2}\int_{-b}^{0} P^S(z')\sum_{n=1}^{\infty}\frac{\psi_n(z)\psi_n(z')}{k_n N_n h(1+\coth k_n a)}\,dz'. \tag{89}$$

Better still, we note that we can write

$$\psi_n(z) = \frac{1}{k_n}\left(\frac{d}{dz}+1\right)\chi_n(z) \tag{90}$$

where

$$\chi_n(z) = \sin k_n z \tag{91}$$

an identity which is established using the dispersion relation. The identity (90) holds for $n=0$ with $k_0 = -\mathrm{i}k$ so that

$$\psi_0(z) = \frac{1}{k}\left(\frac{d}{dz}+1\right)\chi_0(z) \tag{92}$$

and

$$\chi_0(z) = \sinh kz. \tag{93}$$

Noting that $P^S(-b)=0$ and $\chi_n(0)=0$ and integrating by parts leads us to the relation

$$\int_{-b}^{0} P^S(z)\psi_n(z)\,dz = -\frac{1}{k_n}\int_{-b}^{0} V^S(z)\chi_n(z)\,dz \tag{94}$$

where we have defined

$$V^S(z) = \left(\frac{d}{dz}-1\right)P^S(z). \tag{95}$$

This new function has the property that $V^S(0)=0$ since ϕ^S – and hence P^S – satisfies the free surface condition either side of the barrier. It is also important to note that since $P^S(z)\sim O((b+z)^{1/2})$ as $z\to -b^+$ it follows that $V^S(z)\sim O((b+z)^{-1/2})$ as $z\to -b^+$.

We can now write (88) as

$$\left(\frac{d}{dz}+1\right)\mathcal{F}(z) = 0, \qquad -b<z<0 \tag{96}$$

where

$$\mathcal{F}(z) \equiv (\mathcal{M}V^S)(z) + \mathrm{i}(1-R^S)\chi_0(z) \tag{97}$$

and we have written

$$(\mathcal{M}V^S)(z) = \int_{-b}^{0} V^S(z')\mu(z,z')\,dz'; \qquad \mu(z,z') = \sum_{n=1}^{\infty}\frac{\chi_n(z)\chi_n(z')}{N_n k_n h(1+\coth k_n a)}. \tag{98}$$

The solution of (97) with $\mathcal{F}(0)=0$ is obviously just $\mathcal{F}(z)\equiv 0$ for $-b<z<0$. Thus, the result of the manipulations above has been to transform (88) into the integral equation

$$(\mathcal{M}V^S)(z) = -\mathrm{i}(1-R^S)\chi_0(z), \qquad -b<z<0. \tag{99}$$

in which $V^S(0)=0$ and $V^S(z)\sim O((b+z)^{-1/2})$ as $z\to -b^+$.

Returning to (86) and using (92) and integrating by parts gives

$$N_0 kh[\mathrm{i}(1-R^S)\cot ka-(1+R^S)] = -\int_{-b}^{0} V^S(y)\chi_0(z)\,dz. \tag{100}$$

In order to complete the solution we let $v_2(z)$ satisfy the general equation

$$(\mathcal{M}v_i)(z) = g_i(z), \qquad -b<z<0 \tag{101}$$

with $i=2$ where $g_2(z)\equiv\chi_0(z)$; it then follows that

$$V^S(z) = -\mathrm{i}(1-R^S)v_2(z) \tag{102}$$

satisfies (99). Substituting (102) into (100) and rearranging for R^S gives

$$R^S = -\frac{1-\mathrm{i}(\cot ka-\mathsf{T}_{22})}{1+\mathrm{i}(\cot ka-\mathsf{T}_{22})} \tag{103}$$

where, at the moment, we only need one element of the 2×2 matrix T with entries

$$\mathsf{T}_{ij} = \frac{1}{khN_0}\int_{-b}^{0} v_i(z)g_j(z)\,dz. \tag{104}$$

Comparison of (103) with (56) shows that $\mathsf{S}_{22}=\mathsf{T}_{22}^{-1}$.

We remark that the theory of [17] can be applied here since $\mathcal{K}$ and $\mathcal{M}$ are real, symmetric, positive operators. This allows us to say that numerical approximations to S_{22} and T_{22}^{-1} underpinned by a variational method (our choice is Galerkin's method) form lower and upper bounds on the true values of S_{22}, T_{22}^{-1}. The argument is also laid out in [4].

The solution to the radiation problem requires a more subtle approach and we start by writing the potential differently. That is, we opt to write

$$\phi^R(x,z) = \phi^P(x,z)+\tilde{\phi}^R(x,z) \tag{105}$$

where

$$\left(1-\frac{d}{dz}\right)\phi^P(x,0) = \begin{cases} 0, & x<0 \\ 1, & 0<x<a \end{cases} \tag{106}$$

and $\nabla^2\phi^P=0$ in $x<a$, $-h<z<0$ with $\phi^P_x(a,0)=\phi^P_z(x,-h)=0$. As a consequence

$$\phi^P \sim A^P\mathrm{e}^{-\mathrm{i}kx}\psi_0(z), \qquad x\to-\infty \tag{107}$$

where the value of A^P is given by (146) alongside the complete explicit solution for $\phi^P(x,z)$ found in Appendix A.

The remainder of the potential can be expanded as

$$\tilde{\phi}^R(x,z) = \tilde{A}^R\mathrm{e}^{-\mathrm{i}kx}\psi_0(z)+\sum_{n=1}^{\infty}\tilde{a}_n^R\mathrm{e}^{k_nx}\psi_n(z) \tag{108}$$

in $x<0$ and

$$\tilde{\phi}^R(x,z) = -\mathrm{i}\tilde{A}^R\frac{\cos k(x-a)}{\sin ka}\psi_0(z)-\sum_{n=1}^{\infty}\tilde{a}_n^R\frac{\coth k_n(x-a)}{\sinh k_na}\psi_n(z) \tag{109}$$

in $0 < x < a$. It follows that

$$\phi^R(x,z) \sim A^R \mathrm{e}^{-\mathrm{i}kx}\psi_0(z), \qquad x \to -\infty \tag{110}$$

where

$$A^R = A^P + \tilde{A}^R. \tag{111}$$

We note that since ϕ^P is continuous in $z < 0$

$$\begin{aligned}\left[\phi^R\right]_{x=0^-}^{x=0^+} = \left[\tilde{\phi}^R\right]_{x=0^-}^{x=0^+} &= \tilde{A}^R(1+\mathrm{i}\cot ka)\psi_0(z) + \sum_{n=1}^{\infty}\tilde{a}_n^R(1+\coth k_n a)\psi_n(z) \\ &= \begin{cases} P^R(z), & -b < z < 0, \\ 0, & -h < z < -b. \end{cases}\end{aligned} \tag{112}$$

Application of the orthogonality condition (37) then gives

$$\tilde{A}^R(1+\mathrm{i}\cot ka)N_0 h = \int_{-b}^{0} P^R(z)\psi_0(z)\,dz \tag{113}$$

and

$$\tilde{a}_n^R(1+\coth k_n a)N_n h = \int_{-b}^{0} P^R(z)\psi_n(z)\,dz. \tag{114}$$

Imposition of the barrier condition implies that

$$\left.\frac{\partial\tilde{\phi}^R}{\partial x}\right|_{x=0} = -\left.\frac{\partial\phi^P}{\partial x}\right|_{x=0} \tag{115}$$

for $-b < z < 0$ which leads to

$$\sum_{n=1}^{\infty}\frac{k_n\psi_n(z)}{N_n h(1+\coth k_n a)}\int_{-b}^{0}P^R(z')\psi_n(z')\,dz' = \mathrm{i}k\tilde{A}^R\psi_0(z) - \left.\frac{\partial\phi^P}{\partial x}\right|_{x=0}. \tag{116}$$

In order to proceed from here, we perform the same transformation as demonstrated in the scattering problem so that (116) can be made equivalent to

$$(\mathcal{M}V^R)(z) = g_1(z) - \mathrm{i}A^R g_2(z), \tag{117}$$

after use of (148), (111) for $-b < z < 0$ where the operator $\mathcal{M}$ is defined by (88) and $g_2(z) = \chi_0(z)$, as before, $g_1(z)$ is defined by (149). Also

$$V^R(z) = \left(\frac{d}{dz} - 1\right)P^R(z) \tag{118}$$

satisfying $V^R(0) = 0$ (this has only happened because of the factorisation of ϕ^P from the potential from the outset) and $V^R(z) \sim O((z+b)^{-1/2})$ as $z \to -b^-$.

Allowing $v_1(z)$ to be defined by (101) with $i = 1$ implies that

$$V^R(z) = v_1(z) - \mathrm{i}A^R v_2(z). \tag{119}$$

satisfies (117). Using this definition in (113) gives, after use of (104)

$$\tilde{A}^R(1 + \mathrm{i}\cot ka) = \mathrm{i}A^R\mathsf{T}_{22} - \mathsf{T}_{12} \tag{120}$$

and so, from (113), (146) and (111)

$$A^R = \frac{c_0 - \mathsf{T}_{12}}{1 + \mathrm{i}(\cot ka - \mathsf{T}_{22})} \tag{121}$$

where $c_0 = \tanh kh/(N_0 kh)$ is given by (147).

Comparing with (61) shows that there is a relationship, namely $\mathsf{S}_{12} = (c_0 - \mathsf{T}_{12})/\mathsf{T}_{22}$, between the off-diagonal elements of S and T.

We continue by deriving expressions for the other hydrodynamic coefficients of the problem in terms of elements of T. Using $\phi^S(x,z)$ and $\phi^P(x,z)$ in Green's identity applied to the fluid domain bounded by the barrier, wall, bottom, free surface and a vertical boundary through the fluid far to the left of the origin results in

$$q^S = 2\mathrm{i}A^P k \int_{-h}^{0} \psi_0^2(z)\, dz - \int_{-b}^{0} P^S(z)\, \frac{\partial \phi^P}{\partial x}\bigg|_{x=0} dz. \tag{122}$$

which leads to

$$q^S = 2\mathrm{i}A^P khN_0 - \mathrm{i}(1 - R^S) \int_{-b}^{0} v_2(z) \left(g_1(z) - \mathrm{i}A^P g_2(z)\right)\, dz. \tag{123}$$

A considerable amount of algebra simplifies this result to

$$q^S = \frac{2\mathrm{i}khN_0(c_0 - \mathsf{T}_{21})}{1 + \mathrm{i}(\cot ka - \mathsf{T}_{22})} \tag{124}$$

which satisfies (71) with (121).

A similar application of Green's Identity to $\phi^R(x,z)$ and $\phi^P(x,z)$ gives

$$q^R = \int_0^a \frac{\partial \phi^P}{\partial z}\bigg|_{z=0} dx - \int_{-b}^{0} P^R(z)\, \frac{\partial \phi^P}{\partial x}\bigg|_{x=0} dz. \tag{125}$$

which we can write, after transforming variables and integrating by parts, as

$$q^R = \Gamma + \int_{-b}^{0} V^R(z) \left(g_1(z) - \mathrm{i}A^P g_2(z)\right)\, dz \tag{126}$$

Here, using conservation of mass,

$$\Gamma = \int_{-h}^{0} \frac{\partial \phi^P}{\partial x}\bigg|_{x=0} dz = -\frac{\mathrm{i}khN_0 c_0^2}{(1 + \mathrm{i}\cot ka)} + \sum_{n=1}^{\infty} \frac{N_n c_n^2 k_n h}{(1 + \coth k_n a)} \tag{127}$$

where (149), (147) have been used. Then, using (119) we find

$$q^R = \Gamma + khN_0 \left[\mathsf{T}_{11} - \mathrm{i}A^P\mathsf{T}_{12} - \mathrm{i}A^R\mathsf{T}_{21} - A^P A^R\mathsf{T}_{22}\right]. \tag{128}$$

which is a bit of a mess and can probably be simplified enough to show a relationship between S_{11} and T_{11}. In my code I have to make the $+khN_0$ into $-khN_0$ to get it to work and I've no idea why.

4.1 Numerical approximation

The Galerkin method is used again to approximate solutions $v_i(z)$, $i = 1, 2$ to (101). On account of the end-point behaviour known to be satisfied by $v_i(z)$ we write

$$v_i(z) \approx \sum_{p=0}^{P} \beta_p^{(i)} w_{2p+1}\left(\frac{z}{-b}\right) \tag{129}$$

for $-b < z < 0$ in terms of unknown coefficients $\beta_p^{(i)}$ In (129) P is the truncation parameter and

$$w_{2p+1}(t) = \frac{2(-1)^p}{\pi(1-t^2)^{1/2}} T_{2p+1}(t) \tag{130}$$

define test functions in terms of the orthogonal Chebychev polynomials which are odd about $t = 0$. Application of the Galerkin method results in the numerical system of equations

$$\sum_{p=0}^{P} \beta_p^{(i)} \mathcal{M}_{pq} = G_{q0}^{(i)} \tag{131}$$

for $i = 1, 2$, $q = 0, \ldots P$ with

$$\mathcal{M}_{pq} = \sum_{n=1}^{\infty} \frac{G_{pn}^{(2)} G_{qn}^{(2)}}{k_n h N_n (1 + \coth k_n a)} \tag{132}$$

where

$$G_{pn}^{(2)} = \int_{-b}^{0} w_{2p+1}\left(\frac{z}{-b}\right) \chi_n(z)\, dz = J_{2p+1}[k_n b] \tag{133}$$

which means that, explicitly,

$$\mathcal{M}_{pq} = 4 \sum_{n=1}^{\infty} \frac{\cos^2 k_n h J_{2p+1}[k_n b] J_{2q+1}[k_n b]}{(2k_n h + \sin 2k_n h)(1 + \coth k_n a)}. \tag{134}$$

For $n = 0$ we have

$$G_{p0}^{(2)} = (-1)^p I_{2p+1}[kb] \tag{135}$$

The remaining set of coefficients defining the righ-hand side of (131) are, from (149), (147)

$$G_{p0}^{(1)} = \sum_{n=1}^{\infty} \frac{\tan k_n h G_{pn}^{(2)}}{N_n k_n h (1 + \coth k_n a)} \tag{136}$$

Finally, from (104)

$$\mathsf{T}_{ij} \approx \tilde{\mathsf{T}}_{ij} = \frac{1}{khN_0} \sum_{p=0}^{P} \beta_p^{(i)} G_{q0}^{(j)}, \tag{137}$$

$(i, j = 1, 2)$.

5 Results

First let us show the convergence of the results with increasing truncation parameter P from the two complementary formulations of the problem. We have tabulated the complex values of q^S and q^R found in terms of S-matrices and T-matrices in Table 1 for a typical set of parameters (given in the table caption). The convergence with P is incredibly rapid with only a few terms in the approximation needed in most cases to converge to 5 or more decimal places as shown in Tab. 1. Note that all the results are expressed in terms of original, rather than dimensionless variables, hence why K makes an appearance in (138) and Tab. 1. The small differences seen in the values of q^S and q^R are actually due to inaccuracies in the calculation of the various infinite series needed in each method. Thus, to showcase the converge with P the results shown in Tab. 1 uses 16000 terms in the infinite series to evaluate $\mathcal{K}_{pq}$ and $\mathcal{M}_{pq}$ although typically we find 1000 terms and $P = 2$ is sufficient for 3 decimal place accuracy. There are methods for speeding up the infinite series if required.

P	q^S (S)	q^S (T)	q^R (S)	q^R (T)
0	$-0.19809 + 1.69121\mathrm{i}$	$-0.19697 + 1.69054\mathrm{i}$	$0.14371 - 1.22694\mathrm{i}$	$0.15124 - 1.22580\mathrm{i}$
1	$-0.19695 + 1.68953\mathrm{i}$	$-0.19703 + 1.68953\mathrm{i}$	$0.14553 - 1.22435\mathrm{i}$	$0.14702 - 1.22434\mathrm{i}$
2	$-0.19695 + 1.68953\mathrm{i}$	$-0.19703 + 1.68953\mathrm{i}$	$0.14553 - 1.22436\mathrm{i}$	$0.14622 - 1.22436\mathrm{i}$

Table 1: Convergence of q^S and q^R as a function of P for both formulations of the problem in the case of $a/h = 1$, $b/h = 0.5$, $ka = 1$ (or $Kh = 0.761594$)

In [4] results are shown for various hydrodynamic coefficients and we are not going to repeat the results here apart for one case. In Fig. 2 we show the dimensionless flux due to scattering,

$$|q^S/q^I| = |q^S|/Ka \tag{138}$$

where q^I is the flux integrated over $0 < x < a$ of a progressive incident wave given by $\phi^I = \mathrm{e}^{\mathrm{i}kx}\psi_0(z)$ without interaction with the OWC or the rear wall. We note that in the low frequency limit $|q^S/q^I| \to 2$ and that the curves presented in [4] (Fig. 4) are out by a factor of 2. The reason the low frequency limit is 2 and not 1 is that a low frequency progressive wave reflected by a wall results standing wave amplitude twice that of a progressive wave.

We now focus attention on new results, not shown in [4] which correspond to efficiency, E, of power conversion by a *fixed* turbine design rather than just the curves of maximum efficiency assuming the effect of air compressibility is zero, E_{max}. Because of the form of (20) we write

$$\Lambda = \sqrt{Ka}\tilde{\lambda}_1 - \mathrm{i}Ka\tilde{\lambda}_2 \tag{139}$$

such that

$$\tilde{\lambda}_1 = \rho(g/a)^{1/2}\lambda_1 \tag{140}$$

and $\tilde{\lambda}_1$ encodes the design and operation of the air turbine. For the second term we have written

$$\rho\omega^2\lambda_2 = \frac{\rho V_0\omega^2}{\rho_a c_a^2} = Ka\tilde{\lambda}_2 \tag{141}$$

which accounts for the compressibility of the air so that, for a rectangular air chamber,

$$\tilde{\lambda}_2 = \frac{\rho g H_0}{\rho_a c_a^2} \approx 0.07 H_0 \tag{142}$$

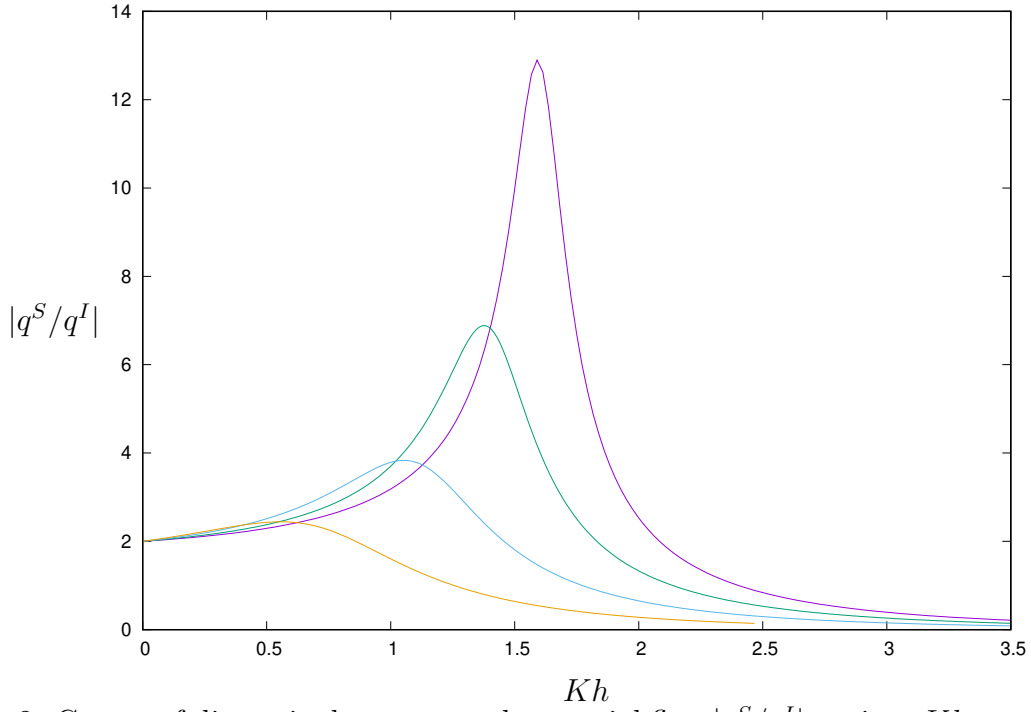

Figure 2: Curves of dimensionless scattered potential flux $|q^S/q^I|$ against Kh corresponding to Fig. 4 of Evans and Porter (1995): $b/h = 0.5$ and $a/h = 0.125,\ 0.25,\ 0.5$ and 1 (progressively reducing in height).

after using physical constants and $H_0 = V_0/a$ is the height of the air chamber.

In Fig. 3 we show the curve of E_{max} for the parameters used in the paper of [14], which forms an envelope over curves of E for different values of $\tilde{\lambda}_1$, assuming $\tilde{\lambda}_2 = 0$ (air compressibility neglected). We already see that theoretically a high-peak efficiency requires a quite careful design of turbine behaviour around $\tilde{\lambda}_1 \approx 1$: if $\tilde{\lambda}_2$ too small or too large there is a drop-off in peak efficiency.

In the paper of [14] the value of H_0 is not given but, based on the pictures in their paper, we have estimated its value at 0.5m. Hence a value of $\tilde{\lambda}_2 = 0.035$ is used in the shown results in Fig. 4. For complex Λ, the theoretical maximum efficiency is 100% and we can just see examples of E exceeding E_{max} in Fig. 4. However, the difference in the results accounting for air compressibility in the experiments is small.

We might imagine a value of $H_0 = 5$m for a full-scale version of the OWC under investigation in X and so in Fig. 5 we show the corresponding results for $\tilde{\lambda}_2 = 0.35$. The curve of E_{max} is now clearly exceeded at higher frequencies.

6 Conclusions

In the paper we have tried to achieve a number of different goals in revisiting the original paper of Evans & Porter [4]. First, we have provided a much more comprehensive and self-contained description of the underlying theory which can hopefully be followed without reverting to textbooks etc. Secondly, we added a complementary method of solution to the existing method of solution outlined in [4]. Thirdly, and perhaps most importantly we have extended the results to show how the efficiency of the two-dimensional rectangular OWC design described by [4]

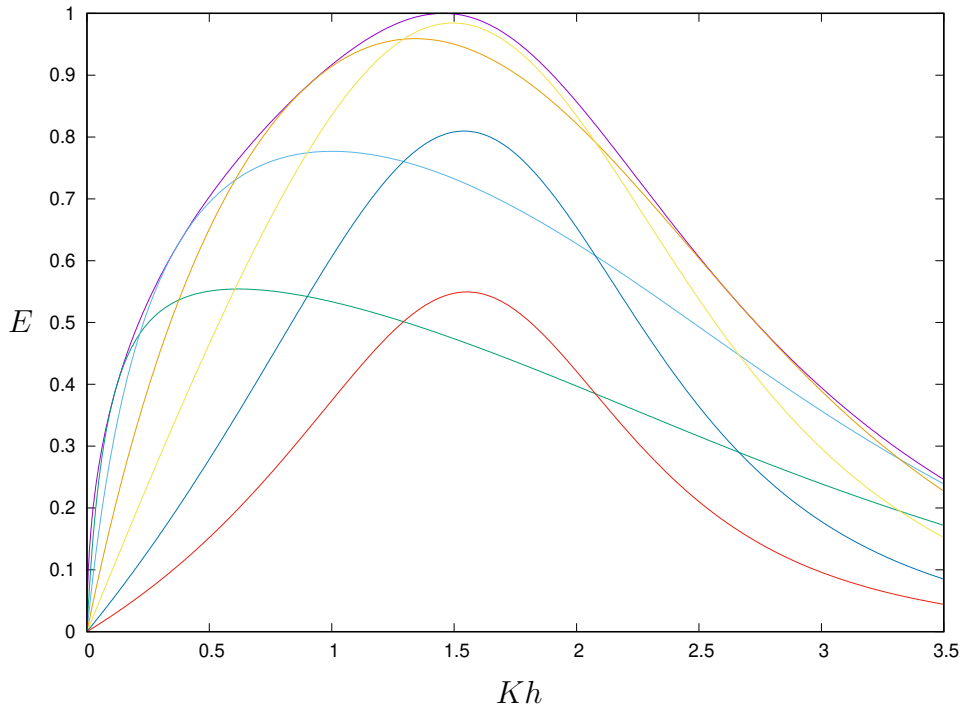

Figure 3: Curves of efficiency against Kh for one of the experiments of Morris-Thomas *et al* (2007) ($a/h = 0.696$, $b/h = 0.25$) for varying $\tilde{\lambda}_1 = 0.25$, 0.5, 1, 2, 4, 8 (progressively left to right) and $\tilde{\lambda}_2 = 0$. All curves sit under the maximum efficiency curve E_{max}.

varies for a fixed turbine design, include the effects of air compressibility rather than just maximum efficiency over all designs without compressible effects. Of particular note is how these efficiencies can be computed using equations (68) and (70) which still rely only upon the real and imaginary parts of a single hydrodynamic coefficient, q^R.

Real fixed turbine modelling may help experimentalists/designers understand their results. We have focussed on the experiments of [14] as a potential means of explaining at least some of the $\sim 30\%$ drop in efficiences reported in their experiments. It is quite possible for the power take-off control parameter, $\tilde{\lambda}_1$ in this paper, to be frequency-dependent and this may also have an influence on how well the predictions fit the experiments.

Appendix A: The potential ϕ^P

We have, in $x < 0$,

$$\phi^P(x,z) = A^P \mathrm{e}^{-\mathrm{i}kx}\psi_0(z) + \sum_{n=1}^{\infty} a_n^P \mathrm{e}^{k_n x}\psi_n(z) \tag{143}$$

and in $0 < x < a$

$$\phi^P(x,z) = 1 - \mathrm{i}A^P \frac{\cos k(x-a)}{\sin ka}\psi_0(z) - \sum_{n=1}^{\infty} a_n^P \frac{\cosh k_n(x-a)}{\sinh k_n a}\psi_n(z) \tag{144}$$

which ensures continuity of velocity across $x = 0$, so that

$$\left.\frac{\partial \phi^P}{\partial x}\right|_{x=0} = -\mathrm{i}kA^P\psi_0(z) + \sum_{n=1}^{\infty} a_n^P k_n \psi_n(z) \tag{145}$$

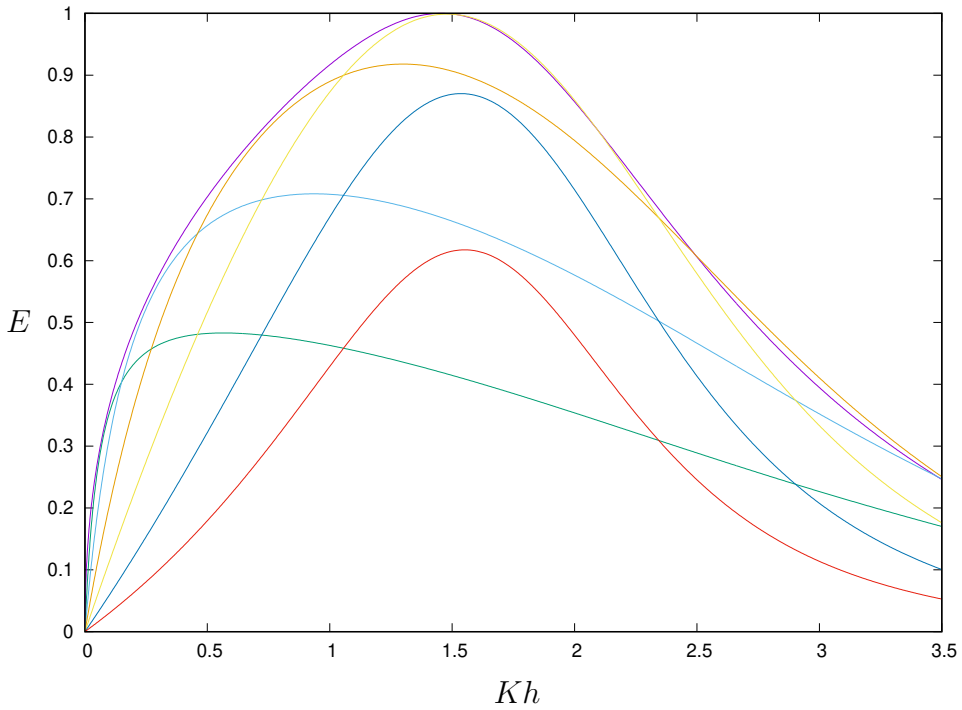

Figure 4: Curves of efficiency against Kh for one of the experiments of Morris-Thomas *et al* (2007) ($b/h = 0.696$, $a/h = 0.25$) for varying $\tilde{\lambda}_1 = 0.25,\ 0.5,\ 1,\ 2,\ 4,\ 8$ (progressively left to right) and $\tilde{\lambda}_2 = 0.035$. For reference, the magenta curve is E_{max} corresponding to $\tilde{\lambda}_2 = 0$.

and the coefficients ensuring continuity of pressure are defined as

$$A^P = \frac{c_0}{(1 + \mathrm{i}\cot ka)}, \qquad a_n^P = \frac{c_n}{(1 + \coth k_n a)} \tag{146}$$

where c_n are the expansion coefficients of the function 1, or

$$c_n = \frac{1}{N_n h}\int_{-h}^{0} \psi_n(z)\,dz = \frac{\tan k_n h}{N_n k_n h}. \tag{147}$$

We have that

$$\left.\frac{\partial \phi^P}{\partial x}\right|_{x=0} = \left(\frac{d}{dz} + 1\right)\left(-\mathrm{i}A^P\chi_0(z) + g_1(z)\right) \tag{148}$$

where

$$g_1(z) = \sum_{n=1}^{\infty} \frac{c_n \chi_n(z)}{(1 + \coth k_n a)} \tag{149}$$

using the definitions in (90)–(93). It should be noted that $\phi_x^P(0, z)$ has a logarithmic singularity as $z \to 0$ which is fairly easy to determine by other means, but apparently not well-known.

References

[1] Erdelyi *et al.* (1954) *Tables of Integal Transforms.* McGraw-Hill, New York.

[2] Evans, D.V. (1978) The Oscillating Water Column Wave Energy Device, *IMA J. Appl. Math.*, **22**(4), 423–433.

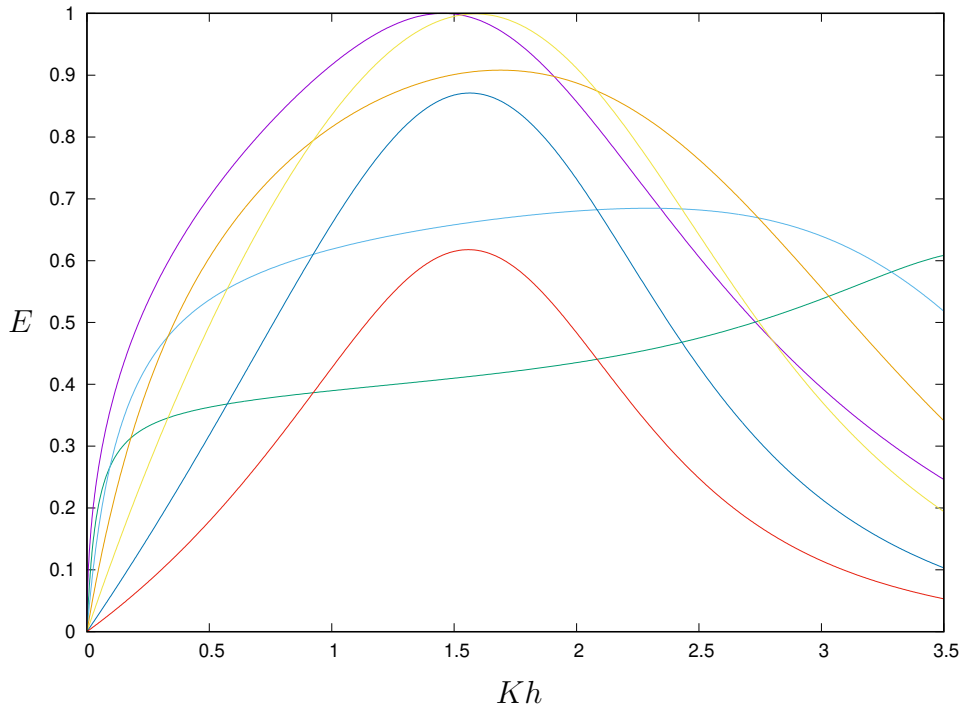

Figure 5: Curves of efficiency against Kh for the geometry of Morris-Thomas *et al* (2007) ($b/h = 0.696$, $a/h = 0.25$) for varying $\tilde{\lambda}_1 = 0.25$, 0.5, 1, 2, 4, 8 (progressively left to right) but with $\tilde{\lambda}_2 = 0.35$ corresponding to a scaled chamber height of 5m. For reference, the magenta curve is E_{max} corresponding to $\tilde{\lambda}_2 = 0$.

[3] Evans, D.V. (1982) Wave-power absorption by systems of oscillating surface pressure distributions. *J. Fluid Mech.,* **114**, 481–499.

[4] Evans, D.V. and Porter, R. (1995) Hydrodynamic characteristics of an oscillating water column device, *Appl. Ocean Res.*, **17**(3), 155–164.

[5] Falcão, A.F. de O. and Sarmento, A.J.N.A. (1980) Wave generation by a periodic surface pressure and its application in wave-energy extraction. *15th Int. Cong. Theor. Appl. Mech.*, Toronto.

[6] Sarmento, A.J.N.A. and Falcão, A.F. de O. (1985) Wave generation by an oscillating surface-pressure and its application in wave-energy extraction. *J. Fluid Mech.,* **150**, 467–485.

[7] Falcão, A.F. de O., Sarmento, A.J.N.A., Gato, L.M.C. and Brito-Melo, A. (2020) The Pico OWC wave power plant: Its lifetime from conception to closure 1986–2018. *Appl. Ocean Res.* **98**, 102104.

[8] Falnes, J. (1993) Research and development in Ocean-wave energy in Norway. *Int. Symp. on Ocean Energy Development* Muroran, Hokkaido, Japan.

[9] Gayathri, R., Chang J.-Y., Tsai, C.-C. and Hsu, T.-W. (2024) Wave energy conversion through oscillating water columns: A review. *J. Marine Sci. Engng.*, **12**(2), 342.

[10] Heath, T.V. (2011) A review of oscillating water columns. *Phil. Trans. Roy. Soc. A.*, **370**(1959), 235–245.

[11] Linton, C.M. and McIver. P. (2001) *Handbook of Mathematical Techniques for Wave/Structure Interactions.* Chapman and Hall/CRC.

[12] Lopez-Mendia, J., Aristondo, A., Ricci, P., Lekube, J., Ceballos, S., and Robles, E. (2025) Improving the power production of Mutriku wave power plant throughout tuning the actual generator and damping valve limits. *Ocean Engng.*, **315**, 119917.

[13] Martin-Rivas, H. and Mei, C.C. (2009) Wave power extraction from an oscillating water column along a straight coast. *Ocean Engng*, **36**(6-7), 426–433.

[14] Morris-Thomas, M.T., Irvin, R.J. and Thiagarajan, K.P. (2007) An Investigation Into the Hydrodynamic Efficiency of an Oscillating Water Column pressure, *J. Offshore Mech. and Arctic Engng.* **129**, 273–278.

[15] Parry Barnard, S. and Porter, R. (2025) The theoretical efficiency of a novel design of Oscillating Water Column with high bandwidth. *In preparation.*

[16] Porter, R. (1995) *Complementary methods and bounds for linear water waves.* Ph.D. thesis, University of Bristol, UK.

[17] Porter, R. and Evans, D.V. (1995) Complementary approximations to wave scattering by vertical barriers. *J. Fluid Mech.*, **294**, 155–180.

[18] Smith, C.M. (1983) *Some problems in linear water waves.* Ph.D. thesis, University of Bristol, UK.